TITLE

Endophyte mediated *Populus trichocarpa* water use efficiency is dependent on time of day and plant water status

AUTHORS (ORCID)

Darshi Banan (0000-0002-9769-7144)

Andrew W. Sher (0000-0002-1594-7673)

Sharon L. Doty (0000-0002-9546-315X)

Soo-Hyung Kim (0000-0003-3879-4080)

School of Environmental and Forest Sciences, College of the Environment, University of Washington, Seattle, WA, USA

Corresponding author and contact: Darshi Banan, dbanan@uw.edu

ABSTRACT

Endophytes are potential partners for improving the resource use efficiency of bioenergy feedstock systems such as short rotation coppiced *Populus.* Endophytes isolated from members of the *Salicaceae* family have broad host compatibility and can improve water use efficiency (WUE) through decreases in stomatal conductance. However, the literature is inconsistent with regards to the environmental conditions and temporal patterns of these benefits. This study investigates how endophyte mediated changes in *Populus trichocarpa* (Torr. and Gray) 'Nisqually-1' stomatal conductance and WUE shift with time and scale in response to water-deficit stress. Leaf gas-exchange and aboveground productivity were used to evaluate the carbon and water balances of glasshouse grown plants in response to endophyte inoculation and water-deficit. Differences in stomatal conductance between control and inoculated plants were

more pronounced (39.7 % decrease, Welch's two-sample t(14.34 df_{adj}) = -2.358, p-value = 0.033) under water-deficit conditions in the late morning during a period of higher light intensity. The decrease in stomatal conductance accompanied a substantial increase in intrinsic WUE (iWUE) for water-deficit inoculated plants. However, increases in iWUE did not result in improvements in aboveground productivity or shoot biomass WUE (WUE_{sb}) for water-deficit inoculated plants. This decoupling between iWUE and aboveground productivity may be an indicator of assimilate allocation to microbial metabolism as an additional carbon sink or a shift in carbon allocation towards belowground biomass. Future work should take a whole-plant approach that accounts for diurnal patterns in incident irradiance to evaluate the impact of endophyte inoculation on host WUE and stress tolerance.

KEYWORDS

Endophytes, *Salicaceae, Populus trichocarpa,* water use efficiency, gas-exchange, water deficit, drought, stomatal conductance, productivity, bioenergy, sustainability, plant microbiome, climate change

INTRODUCTION

Members of the plant genus *Populus* are ideal candidates for short rotation coppice systems planted on marginal lands to sustainably produce bioenergy feedstocks (Tuskan 1998). To maximize sustainability, careful consideration must be given to the resource use efficiency and biogeochemical outcomes of these production systems and requires a broad assessment of plant genotype, ecosystem interactions, and management practices (Davis et al. 2013). With a wide distribution across latitudes, elevations, and watersheds, the model tree species, *Populus trichocarpa,* is a diverse

genetic resource with equally diverse phenotypes (Gornall and Guy 2007; Mckown, Guy, et al. 2014; Holliday et al. 2016; Chhetri et al. 2019; Liu and El-Kassaby 2019; Zhang et al. 2019). This diversity has been used to develop mapping populations and generate hybrids with other members of genus *Populus* for enhanced biomass productivity under managed settings (Bunn et al. 2004; McKown and Guy 2018; Ahmed et al. 2020). Natural variation in traits underlying water use efficiency (WUE) such as stomatal patterning, stomatal conductance, and mesophyll conductance may be selected upon to further improve the resource use efficiency of *Populus* (Soolanayakanahally et al. 2009; Mckown, Klápště, et al. 2014). However, breeding for improved WUE remains difficult due to biophysical limitations in the exchange of CO_2 for H_2O through stomata as well as tradeoffs between stomatal conductance and disease resistance (Leakey et al. 2019; McKown et al. 2019).

Inoculation with endophytes, beneficial microbes that live inside plant hosts, can potentially alleviate breeding bottlenecks and expand the range of plant phenotypic plasticity especially in response to our rapidly changing climate (Weyens et al. 2009; Nogales et al. 2016; Bell et al. 2019). Diverse endophytes have been shown to provide a wide range of plant hosts with benefits including enhanced nutrient acquisition, increased rooting, pest and pathogen defense, improved abiotic stress response, and general increases in productivity (Liu et al. 2017; Rho, Hsieh, et al. 2018). In exchange, host plants provide a suitable growth environment, primarily in intercellular spaces, and supply carbohydrates, amino acids, and inorganic nutrients (Kandel et al. 2017). The outcomes of plant-microbe interactions are highly context dependent and can shift between positive, neutral, or negative with different combinations of host genotype,

microbe community composition, and environmental conditions (Sapp 2004; Trivedi et al. 2020). Therefore, understanding the mechanisms underlying these interactions is necessary to fully utilize this symbiotic relationship in plant production systems and to make accurate predictive models that can inform the role of endophytes in management, conservation, and phytoremediation strategies.

Members of the family *Salicaceae,* which includes *P. trichocarpa* and *Salix sitchensis,* are also associated with endophyte communities. *Salicaceae* associated endophytes occur as communities that vary with the geography and climates of their host origin (Firrincieli et al. 2020). Under controlled conditions, endophytes isolated from *Salicaceae* have been shown to improve host productivity, tissue nitrogen content, phosphorous solubilization, drought stress resilience, and soil pollutant degradation relative to non-inoculated control plants (van der Lelie et al. 2009; Knoth et al. 2014; Khan et al. 2016; Doty et al. 2017; Varga et al. 2020). In addition to benefiting their original isolate hosts, endophytes isolated from *Salicaceae* also have demonstrated cross species host compatibility and growth promotion in diverse hosts including *Zea mays, Solanum lycopersicum, Lolium perenne,* and *Pseudotsuga menziesii* (Khan et al. 2012; Knoth et al. 2013; Kandel et al. 2015; Khan et al. 2015; Rho, van Epps, et al. 2018). This broad host range suggests that curated endophyte communities may be a valuable tool for accelerating plant improvement and climate change adaptation.

Various mechanisms may explain how endophyte communities potentially benefit their host. Diazotrophic endophytes such as WP5 (*Rahnella aceris*) and WPB (*Burkholderia vietamiensis*) are able to fix atmospheric N_2 (Varga et al. 2020; Doty et al. 2009; Xin, Glawe, et al. 2009; Firrincieli et al. 2015). Up to 65 % of the nitrogen used by

hybrid poplar clone ‘H11-11’ (*Populus trichocarpa* x *Populus deltoides*) grown under low nitrogen conditions was provided by diazotrophic endophytes (Knoth et al. 2014). Many strains are capable of producing phytohormones *in vitro* such as salicylic acid, jasmonic acid, indole acetic acid (IAA), abscisic acid (ABA), gibberellins, and brassinosteroids which prime and modify plant responses to biotic and abiotic stress (Khan et al. 2016). Strains such as WP1 (*Rhodotorula graminis*) and PDN3 (*Enterobacter* asburiae) are high IAA producers. Endophyte genome sequencing has identified putative genes related to abiotic stress tolerance (Firrincieli et al. 2015) . Under drought stress, hybrid poplar ‘OP367’ (*Populus deltoides x Populus nigra)* and *Oryza sativa* ‘M-206’ inoculated with *Salicaceae* endophytes have been shown to reduce stomatal conductance, sustain photosynthesis, and increase root-to-shoot ratio (Khan et al. 2016; Rho, van Epps, et al. 2018).

The physiological impacts of plant-endophyte interactions may vary with time of day. In particular, stomatal conductance patterns throughout the day are mediated by osmolyte and phytohormone trends, both of which may be modified by endophyte activity (Kandel et al. 2017; Kumar et al. 2020). Khan et al. (2016) and Rho et al. (2018) observed the greatest differences in stomatal conductance between non-inoculated and inoculated hybrid poplar and rice in the late afternoon but did not report diurnal patterns of light intensity. While the decreases in stomatal conductance observed in Rho et al. (2018) with rice did not correspond with an increase in intrinsic WUE, they did result in an improvement to biomass WUE at harvest. Studies of *Lolium arundinaceum* infected with fungal endophytes have also observed reductions in stomatal conductance in

response to inoculation but did not track diurnal light trends or relate changes in leaf gas-exchange to productivity (Elmi et al. 1995; Swarthout et al. 2009).

Due to the wide variety of host systems, environments, stresses, and times of day investigated throughout the plant-endophyte literature, it can be difficult to effectively maximize the potential benefits and applications of plant-endophyte interactions. This study uses a consortium of endophytes originally isolated from *Salicaceae* to inoculate a model tree species, *Populus trichocarpa (*Torr. and Gray) 'Nisqually-1', closely related to the natural host system. As it is unlikely that a single strain will provide complete drought tolerance to host plants, a consortium of selected strains is employed. Previous data with a 10-strain consortium in hybrid poplar 'OP367' (*Populus deltoides x Populus nigra)* and a 12-strain consortium in *Pseudotsuga menziesii* conferred drought tolerance to the host plants (Khan et al. 2015; Khan et al. 2016). For this study, we sought to narrow down to 5 strains based on commonality between the previous consortia, on genomic analysis for presence of genes known to be involved in stress tolerance, and on results from field tests (Doty et al. 2017). This study seeks to: (1) assess the temporal pattern of how endophytes mediate the gas-exchange response to water deficit, and (2) determine if changes in leaf level intrinsic WUE (iWUE) correspond with changes in aboveground productivity and shoot biomass WUE (WUE_{sb}). By using WUE to screen for the endophyte consortium's effectiveness, this study tests the hypotheses that differences in stomatal conductance are greater when light is highest, endophyte inoculated plants have higher iWUE, and endophyte inoculated plants have higher productivity compared to non-inoculated plants grown under water-deficit.

METHODS

Endophyte strains and inoculum preparation

The inoculum included five endophyte strains, WPB, WP5, WW5, WP1, and PDN3, selected for their ability to fix N_2 and enhance host productivity and abiotic stress resistance (Table 1). For inoculum preparation, each strain was grown in 10 ml MG/L broth (Cangelosi et al. 1991) without biotin (per liter: 5 g tryptone, 2.5 g yeast extract, 5.2 g sodium chloride, 10 g mannitol, 2.32 g sodium glutamate, 0.5 g potassium phosphate monobasic, and 0.2 g magnesium sulfate heptahydrate). Strains were grown with shaking at 30 ^{o}C overnight, and cells harvested by centrifugation at 6000 g at 4 ^{o}C for 10 minutes before being resuspended in approximately 2 ml nitrogen free media (NFM, Doty et al. 2009). Optical densities (OD_{600}) were assessed for each of the 5 strains, and each concentrated suspension was diluted to an OD_{600} of 0.1 using NFM. Equal volumes of each adjusted suspension were then mixed to produce an inoculum with an overall OD_{600} of 0.1 with each strain equally represented.

Plant materials, growth conditions, and treatment application

The experiment was conducted in between day of year (DOY) 73 and DOY 127 2021 at the Douglas Research Conservatory at the University of Washington, Seattle. Forty tissue culture-grown, internally sterile *Populus trichocarpa* (Torr. and Gray) 'Nisqually-1' 8 week old rooted clones were used as host plants. After one day in ½ strength Hoagland's solution (Hoagland and Arnon 1950) to rinse off adhering agar, 20 plants were randomly selected for transfer to 50ml beakers containing 20 ml of the inoculum. To maintain the axenic conditions, the beakers with the plants were maintained in sterile Magenta vessels (Caisson Labs, Smithfield, UT, USA). The

remaining 20 plants were mock-inoculated in NFM in Magenta vessels. Five days after inoculation (DAI), plants were transplanted into 840 ml pots (Dillen Products, Middlefield, OH, USA) each containing an average of 270 g of air-dried Sunshine Mix #2 (Sun Gro Horticulture, Agawam, MA, USA), wetted with deionized water, and placed under a mist tent to promote establishment for one week. The plants were then arranged in a randomized complete block design with 10 complete blocks under a glasshouse where they experienced an average 21 ^{o}C temperature, 58 % relative humidity, and a 14/10 hour light/dark photoperiod from supplemental LED lamps (ZELION HL300 Grow White, OSRAM Sylvania Inc., Wilmington, MA, USA). Plants were fertigated with a 175 ppm 17-17-17+ Nutriculture liquid nutrient solution (Plant Marvel Laboratories Inc., Chicago Heights, IL, USA) and the amount of water or nutrient solution added to the pots was recorded throughout the experiment.

Pots were placed on saucers to minimize cross-contamination of endophyte treatments through watering run-off. Portions of measurement equipment that contacted plant tissue or potting media were disinfected with 70 % ethyl alcohol. Nitrile gloves were worn for plant handling and were changed between endophyte treatments.

23 DAI, 10 mock-inoculated and 10 endophyte-inoculated plants were randomly assigned to undergo water-deficit treatment while the remaining plants continued to receive well-watered conditions. The target well-watered condition was 85 % of pot water holding capacity and the target water-deficit condition was 33 % of pot water holding capacity. Pot moisture content was determined by weighing pots every 2-3 days and converted to a percentage of water holding capacity using the ratio of oven-dried media weight to the weight of potting media at full water holding capacity. The

contribution of plant tissue to the pot system's weight was assumed to be negligible. These values were used to determine the amount of water or nutrient solution necessary to maintain the pot at a target water holding capacity for the well-watered and water-deficit treatments. At each watering event, water was added slightly in excess of the 85 % and 33 % targets such that the average WHC throughout the treatment duration was near these targets. The water holding capacity of water-deficit pots plateaued at 40 DAI and was maintained at an average of 35.3 ± 0.7 % for an additional 14 days until destructive harvest (Figure 1A). Well-watered pots were maintained at an average of 80.6 ± 1.9 % of water holding capacity during the period of differential irrigation. In total, each well-watered plant received an average of 1670 ml of irrigation and each water-deficit plant received an average of 660 ml of irrigation over the course of the experiment (Figure 1B). To determine water holding capacity, a test set of pots containing air dried media was weighed and then brought to saturation. The pot tops were sealed to prevent water loss through evaporation, allowed to percolate with gravity for three days, weighed to determine pot water holding capacity, placed in a 65 ^{o}C oven for one week, and weighed once more. The initial weight of air-dried media in each experimental pot was recorded and the ratio between air-dried and oven-dried media weight was used to convert the pot's wet weight to a percentage of water holding capacity. Empty pot weights were not tracked to account for soil evaporation. Changes in pot weight between irrigations were the result of total evapotranspiration. Potential differences in soil evaporation between treatments were not specifically examined.

Measurements

Diurnal time course measurements of stomatal conductance to water vapor (g_{sw}, mol m^{-2} s^{-1}) and light-adapted chlorophyll fluorescence (ΦPSII) were collected using a LI-600PF porometer/fluorometer (LI-COR Biosciences, Lincoln, NE, USA). Measurements were collected on 45 DAI at 2-hour intervals between 08:00 and 16:00 (hh:mm) from the youngest fully expanded leaf from all replicates (n = 10). These diurnal measurements were used to determine the time of day where differences in stomatal conductance and chlorophyll fluorescence between endophyte treatments were most pronounced.

The chlorophyll content of the youngest fully expanded leaf on each plant was estimated on 46 DAI using a SPAD 502 hand-held chlorophyll meter (Konica Minolta Sensing Americas Inc., Ramsey, NJ, USA). Plant height (mm) was measured on 54 DAI as the distance between the base of the plant and the shoot apical meristem on the main axis of the plant.

Survey leaf gas-exchange measurements were collected from the youngest fully expanded leaf on each plant in seven blocks (n = 7) on 54 DAI at 10:00 using a LI-6800 portable photosynthesis system (LI-COR Biosciences, Lincoln, NE, USA). Net CO_2 assimilation rate (A_n, μmol m^{-2} s^{-1}) and stomatal conductance (g_{sw}, mol m^{-2} s^{-1}) were calculated according to the equations of Farquhar, von Caemmerer, and Berry (1980). The conditions inside the gas-exchange measurement cuvette were set to match ambient conditions at the time of collection, with a light intensity of 500 μmol m^{-2} s^{-1}, a relative humidity of 60 %, and a block temperature of 25 ^{o}C. The [CO_2] of the air flowing into the cuvette was set to 400 μmol mol^{-1}. A_n and g_s were used to calculate intrinsic water use efficiency *(*A_n / g_s = iWUE*,* μmol mol^{-1}).

Immediately following leaf gas-exchange measurements, the measured leaf was removed and imaged for area estimation (ImageJ, NIH, Bethesda, MD, USA) using a copy stand equipped with a Nikon d5300 DSLR camera (Nikon USA Inc., Melville, NY, USA). The leaf was then dried at 65 ^{o}C for 72 hours and weighed to determine specific leaf area (SLA, $mm^2\ mg^{-1}$). The aboveground tissue of each plant was harvested on 54 DAI, dried at 65 ^{o}C for 72 hours, weighed, and summed with the weight of the leaf sampled for SLA to determine aboveground biomass productivity. Dry aboveground biomass and the total volume of water or nutrient solution supplied to the pots were used to estimate shoot biomass water use efficiency (WUE_{sb}, mg L^{-1}). Measurements of SPAD, SLA, aboveground biomass productivity, and WUE_{sb} were collected from all replicates (n = 10).

Statistical analysis

Data were analyzed using R, version 4.0.3 (R Core Team 2021). Orthogonal contrasts were performed using a two-sample Welch's t-test between non-inoculated and endophyte inoculated treatments within each well-watered and water-deficit condition. The adjusted degrees of freedom (df_{adj}), t-statistic, and p-value are reported. In addition, to test inoculation and irrigation treatment effects and their interactive effect, a two-way analysis of variance (ANOVA) using aov() in base R was performed on two factors each with two levels resulting in four treatment combinations: Well-watered Control, Well-watered Inoculated, Water-deficit Control, Water-deficit Inoculated. Blocks were treated as a fixed effect in the model. The assumption of homogeneity of variances was assessed with the Levene's test using the 'car' package in R (Weisberg 2019). For repeated measures of g_s and $\Phi PSII$, - both the orthogonal contrasts and

two-way ANOVA was performed at each timepoint. Data were visualized using the R package 'ggplot2' (Whickham 2016).

RESULTS

Diurnal measurements of stomatal conductance and ΦPSII were collected on 45 DAI. Over the course of the day, stomatal conductance was consistently lower in water-deficit plants compared to well-watered plants regardless of inoculation treatment (ANOVA: df = 1, p-value < 0.001, Figure 2A, Supplemental Table 1). At 08:00, inoculated plants had 10 % greater stomatal conductance than non-inoculated plants under well-watered conditions (Welch's two sample t(17.95 df_{adj}) = 2.71, p-value = 0.015). At 10:00, inoculated plants had 39.7 % lower stomatal conductance than non-inoculated plants under water-deficit (Welch's two-sample t(14.34 df_{adj}) = -2.358, p-value = 0.033) and 9.5 % lower stomatal conductance under well-watered conditions (Welch's two-sample t(16.48 df_{adj}) = -2.21, p-value = 0.042). All plants had similar ΦPSII values between 08:00 and 10:00 (ANOVA: df = 1, p-value > 0.05, Figure 2B, Supplemental Table 2). Between 12:00 and 16:00, water-deficit plants had significantly lower ΦPSII than well-watered plants regardless of inoculation treatments (ANOVA: df = 1, p-value < 0.01). PPFD was greatest (average value = 535.65 μmol m^{-2} s^{-1}) at the 10:00 timepoint (Figure 2C).

Survey leaf gas-exchange measurements were collected beginning at 10:00 on 54 DAI. Water-deficit plants had lower rates of assimilation and stomatal conductance than well-watered plants in both inoculation treatments (ANOVA: df = 1, p-value < 0.001, Figure 3A; ANOVA: df = 1, p-value < 0.001, Figure 3B; Supplemental Table 3). Under water-deficit conditions, inoculated plants had significantly lower stomatal

conductance than non-inoculated plants (Welch's two-sample t(9.0355 df_{adj}) = -2.4, p-value = 0.038), Figure 3B) and significantly greater intrinsic water use efficiency (iWUE, Welch's two-sample t(5.4113 df_{adj}) = 2.64, p-value = 0.043, Figure 3C)..

Under water-deficit conditions, leaf chlorophyll content assessed as SPAD values was greater in inoculated plants compared to non-inoculated plants (Welch's two-sample t(17.984 df_{adj}) = 2.7442, p-value = 0.01, Figure 4A). Specific leaf area (SLA) did not respond to inoculation and was greater in well-watered plants than water-deficit plants regardless of inoculation treatment (Figure 4B, Supplemental Table 4). Within each of the water treatments, inoculation did not have an effect on aboveground biomass, plant height, and WUE_{sb}. Regardless of inoculation, aboveground biomass, plant height, and WUE_{sb} were consistently greater in well-watered plants than water-deficit plants (Figure 5, Supplemental Table 4).

DISCUSSION

The endophyte strains used in this study reduced *Populus trichocarpa* stomatal conductance under water-deficit in a time-of-day dependent manner. Photosynthesis assessed by net assimilation rate and ΦPSII were reduced by water-deficit stress but not significantly impacted by endophyte inoculation. The reduction in stomatal conductance accompanied an increase in ¡WUE. However, this improved *iWUE* did not correspond with an improvement in aboveground biomass productivity or WUE_{sb}.

The reduction in stomatal conductance in response to inoculation is consistent with other studies that tested *Salicaceae* endophytes on hybrid poplar clone 'H11-11' (*Populus trichocarpa* x *Populus deltoides*) and *Oryza sativa* 'M-206' as well as tall fescue (*Festuca arundinaceae*) inoculated with a fungal endophyte under drought

conditions (Elmi and West 1995; Swarthout et al. 2009; Khan et al. 2016; Rho et al. 2018). With the exception of Rho et al. (2018), these studies observed stomatal conductance at a single afternoon timepoint. Rho et al. (2018) observed the greatest differences in stomatal conductance between non-inoculated and inoculated plants in the late afternoon. In contrast, in the present study, the impact of endophyte inoculation on stomatal conductance was greatest under water-deficit conditions in the late morning (Figure 2A), during the period of greatest light intensity (Figure 2C).

Multiple mechanisms may contribute to an altered diurnal pattern of stomatal conductance in response to endophyte inoculation. Light influences stomatal conductance via control of stomatal aperture at short time scales (Sharkey and Raschke 1981; Farquhar and Sharkey 1982). Although diurnal courses of light intensity were not reported, in rice inoculated with *Salicaceae* endophytes, the most pronounced differences in stomatal conductance occurred in trials that experienced a greater daily light integral (Rho, van Epps, et al. 2018). Light is needed to produce the common currency of plant-microbe mutualism, photosynthates, and has been shown to modify interactions between plants and their endophytes (Davitt et al. 2010; Heath et al. 2020). Sucrose is a key metabolite that controls stomatal aperture by acting as an osmolyte and an energetic substrate (Talbott and Zeiger 1998; Medeiros et al. 2018; Lima et al. 2018). Endophytes utilize carbohydrates, including sucrose, produced by their host (Kandel et al. 2017; Kumar 2020). This common need for sucrose between both host and endophyte may change the pattern of sucrose concentration throughout the day.

Phytohormones such as ABA and IAA control the development of epidermal patterning and influence stomatal behavior (Balcerowicz and Hoecker 2014; Le et al.

2014). Increased ABA concentration was observed in endophyte inoculated rice plants that also had decreases in stomatal conductance and stomatal density (Rho, van Epps, et al. 2018). *Salicaceae* endophytes have been shown to produce a variety of phytohormones *in vitro* (Khan et al. 2016). The endophytes used in the present experiment were selected in part due to their ability to synthesize ABA and IAA and this may explain the stomatal conductance response to water-deficit seen in inoculated plants. While the current study was performed with a consortium of *Salicaceae* endophytes, further testing of individual strains could help determine the degree to which specific endophytes alter host phytohormone status and modify stomatal patterning and conductance.

Improvements in iWUE by endophyte inoculation under water-deficit conditions appear to be driven by the decrease in stomatal conductance and a maintenance of net assimilation rate. Leaf WUE can be improved by either reducing the ratio between leaf intercellular [CO_2] and atmospheric [CO_2] (leaf intercellular airspace [CO_2] / atmospheric [CO_2], C_i / C_a) or reducing the difference in vapor pressure deficit between the leaf intercellular airspace and the atmosphere (leaf intercellular airspace vapor pressure deficit – atmospheric vapor pressure deficit, W_i - W_a) (Leakey et al. 2019). C_i / C_a can be reduced by increasing intercellular [CO_2] near the site of carboxylation by Rubisco. The nitrogenase enzyme utilized by endophytes to fix N_2 is sensitive to O_2 and it is suspected that the metabolic respiration of sucrose by endophytes creates a microaerobic environment (Doty et al. 2009). Microbial respiration is estimated to provide up to 57 % of the CO_2 assimilated by endophytes inoculated rice (Rho, Doty, et al. 2018). This may contribute to an increased mesophyll conductance and improved

leaf WUE when stomatal conductance is reduced (Flexas et al. 2016). In this way, endophyte N_2 fixation potentially benefits host photosynthesis both by providing nitrogen for Rubisco production and concentrating the substrate for Rubisco carboxylation, even under conditions where stomatal closure may limit [CO_2]. (W_i - W_a) can be reduced by the aforementioned changes in stomatal responsiveness and also by changing canopy architecture such that the microenvironment has reduced vapor pressure deficit. *Salicaceae* endophyte inoculation increased branch number in *Populus* and tiller number in *Oryza sativa* however the impact that these changes may have on the canopy microenvironment is unknown (Knoth et al. 2014; Kandel et al. 2015).

The lack of significant increases in aboveground biomass productivity in the present experiment is in contrast to other *Populus* studies that showed improved growth in response to endophyte inoculation (Taghavi et al. 2009; Rogers et al. 2012; Knoth et al. 2014; Khan et al. 2016). However, these experiments investigated the effect of different endophyte strains and improved biomass productivity may not be a generalizable response. Additionally, the lack of improved biomass productivity may be due in part to this experiment's short duration where destructive biomass harvest occurred only 54 days after inoculation. In a study of *Oryza sativa* inoculated by *Salicaceae* endophytes, inoculated plants were shorter than control plants in the first month of growth but overtook them by the second and fourth months, suggesting a lag before growth benefits accrue (Kandel et al. 2015). The increase in SPAD leaf chlorophyll content of inoculated plants under water-deficit conditions (Figure 4A) and the slight but non-significant productivity stimulations in inoculated plants under well-

watered conditions (Figure 5A,B) suggest a positive trend of small compounding benefits that may take time to become apparent.

The lack of a significant change in aboveground productivity may also be due to an altered host carbon balance as a result of inoculation. Two ways that the host carbon balance may shift in response to inoculation include (1) an increase in root-to-shoot biomass allocation and (2) endophytes acting as a carbon sink. First, an increase in root-to-shoot biomass allocation is a consistent response to *Salicaceae* endophytes observed across several studies with hosts including hybrid *Populus*, *Zea mays*, *Oryza sativa*, and *Pseudotsuga menziesii* grown under control, drought stress, and nitrogen stress conditions (Khan et al. 2012; Knoth et al. 2013; Knoth et al. 2014; Kandel et al. 2015; Khan et al. 2015; Khan et al. 2016). Although some of these studies also reported an increase in aboveground biomass in response to inoculation, that was not the case in the present experiment (Fig 5A). The junctions at the emergence points of root hairs and lateral roots are common entryways for bacterial endophytes (Kandel et al. 2017). Changes in root-to-shoot biomass allocation and root system architecture may have potential benefits for both endophyte colonization and host responses to stress. Root system architecture exhibits wide phenotypic plasticity under stress and an increase in root depth and root length density to areas where water is accessible are favorable responses to drought (Comas et al. 2013; Brunner et al. 2015; Karlova et al. 2021). It should be noted that belowground biomass and root system architecture were not measured in the present study. Future efforts should take advantage of potting medias that are suited to root excavation and make use of image-based root phenotyping techniques to determine the degree to which endophyte inoculation alters root

development. Second, endophytes metabolize photosynthates from their host and this reflects a substantial cost to the plant. However, this can also stimulate rates of photosynthesis due a change in carbon sink strength (Kaschuk et al. 2009; Rho et al. 2020). Because of their influence on the overall carbon and water balance of their host, endophytes may influence how plants respond to stress through changes in hydraulic conductance and carbon starvation (Flexas et al. 2006; Sevanto et al. 2014). Finally, the lack of a significant improvement in aboveground productivity or WUE_{sb} may be due to a weak signal that was not detected with the current study's methods and statistical power.

This experiment and the broader literature show that plant-endophyte interactions are highly context specific. In many cases, endophyte community composition is dependent on sampling site, soil type, environmental conditions, and abiotic stress (Gottel et al. 2011; Timm et al. 2018; Firrincieli et al. 2020; Morales Moreira et al. 2021; Wipf et al. 2021). Even different classes of an abiotic stress, such as acute progressive drought versus cyclic drought, can result in distinct endophyte responses (Garcia et al. 2018). Furthermore, these interactions are sensitive to seasonality and ontogeny (Shakya et al. 2013; Wagner et al. 2016; Ma et al. 2021). Given the complexity of these interactions, it is important to relate host growth and physiology responses to some metric of endophyte colonization. Future studies will incorporate methods such as 16S rRNA sequencing or ddPCR with strain specific primers to characterize endophyte colonization.

Characterizing these complex plant, endophyte, and environment interactions can be aided by combining in-depth ecophysiological and microbiome measurements

with advancements in high-throughput whole-plant phenotyping. A platform that leverages thermal imaging for stomatal behavior, spectral imaging for aboveground productivity and root system architecture, and spectral reflectance indices for endophyte diversity and distribution would provide a more thorough evaluation of carbon budget and water use responses to endophyte inoculation (Sanchez-Azofeifa et al. 2012; Feldman et al. 2017; Mattupalli et al. 2019; Pignon, Fernandes, et al. 2021). The depth and coordination of information from such an approach would better consider endophytes as part of the host's extended physiological phenotype (Whitham et al. 2003; Cregger et al. 2021). By considering the holobiont, endophytes may be parameterized into existing process-based models that utilize leaf gas-exchange, resource partitioning, and canopy structure to predict short rotation coppice *Populus* productivity and realize the impacts endophytes may have on landscape scale resource use and biogeochemical processes (Deckmyn et al. 2004; Amichev et al. 2010; Wang et al. 2013; Morris 2018; Henner et al. 2020).

AUTHOR CONTRIBUTIONS

DB designed and executed the experiment, collected data, analyzed results, and wrote the manuscript. AWS performed plant tissue culture, prepared the microbe consortia, inoculated the plants, summarized microbe traits, and edited the manuscript. SLD acquired funding, performed plant tissue culture, prepared the microbe consortia, inoculated the plants, summarized microbe traits, and edited the manuscript. S-HK acquired funding, designed and supervised the experiment, and edited the manuscript.

ACKNOWLEDGEMENTS

The authors would like to thank Annie Bilotta and David Zuckerman for greenhouse support and Sriram Parasurama for processing samples. We are grateful to Dr. Johan Leveau and two anonymous reviewers for their constructive comments that helped to improve the manuscript. This research was supported by the DOE Office of Science, Office of Biological and Environmental Research (BER), grant number DE-SC0021137.

REFERENCES

Ahmed AKM, Jiang L, Wang F, Chen S, Zhou X, Pei X, Zhao X, Qu G. 2020. Variation analysis of growth traits of four poplar clones under different water and fertilizer management. J For Res. 31(1):45–55. doi:10.1007/s11676-019-00888-y. https://doi.org/10.1007/s11676-019-00888-y.

Amichev BY, Johnston M, Van Rees KCJ. 2010. Hybrid poplar growth in bioenergy production systems: Biomass prediction with a simple process-based model (3PG). Biomass and Bioenergy. 34(5):687–702. doi:10.1016/j.biombioe.2010.01.012. http://dx.doi.org/10.1016/j.biombioe.2010.01.012.

Balcerowicz M, Hoecker U. 2014. Auxin - a novel regulator of stomata differentiation. Trends Plant Sci. 19(12):747–749. doi:10.1016/j.tplants.2014.10.006. http://dx.doi.org/10.1016/j.tplants.2014.10.006.

Bell TH, Hockett KL, Alcalá-Briseño RI, Barbercheck M, Beattie GA, Bruns MA, Carlson JE, Chung T, Collins A, Emmett B, et al. 2019. Manipulating wild and tamed phytobiomes: Challenges and opportunities. Phytobiomes J. 3(1):3–21. doi:10.1094/PBIOMES-01-19-0006-W.

Brunner I, Herzog C, Dawes MA, Arend M, Sperisen C. 2015. How tree roots respond to drought. Front Plant Sci. 6(547):1–16. doi:10.3389/fpls.2015.00547.

Bunn SM, Rae AM, Herbert CS, Taylor G. 2004. Leaf-level productivity traits in Populus grown in short rotation coppice for biomass energy. Forestry. 77(4):307–323. doi:10.1093/forestry/77.4.307.

Cangelosi, Gerard A. EAB, Gladys Martinetti and EWN. 1991. Genetic analysis of Agrobacterium. 204(18):384–397.

Casella E, Ceulemans R. 2002. Spatial distribution of leaf morphological and physiological characteristics in relation to local radiation regime within the canopies of 3-year-old Populus clones in coppice culture. Tree Physiol. 22(18):1277–1288. doi:10.1093/treephys/22.18.1277.

Chhetri HB, Macaya-Sanz D, Kainer D, Biswal AK, Evans LM, Chen JG, Collins C, Hunt K, Mohanty SS, Rosenstiel T, et al. 2019. Multitrait genome-wide association analysis of Populus trichocarpa identifies key polymorphisms controlling morphological and physiological traits. New Phytol. 223(1):293–309. doi:10.1111/nph.15777.

Comas LH, Becker SR, Cruz VM V., Byrne PF, Dierig DA. 2013. Root traits contributing to plant productivity under drought. Front Plant Sci. 4(NOV):1–16. doi:10.3389/fpls.2013.00442.

Cregger MA, Carper DL, Christel S, Doktycz MJ, Labbé J, Michener JK, Dove NC, Johnston ER, Moore JAM, Vélez JM, et al. 2021. Plant-microbe interactions: From genes to ecosystems using populus as a model system. Phytobiomes J. 5(1):29–38. doi:10.1094/PBIOMES-01-20-0009-FI.

Davis SC, Boddey RM, Alves BJR, Cowie AL, George BH, Ogle SM, Smith P, van Noordwijk M, van Wijk MT. 2013. Management swing potential for bioenergy crops.

GCB Bioenergy. 5(6):623–638. doi:10.1111/gcbb.12042.

Davitt AJ, Stansberry M, Rudgers JA. 2010. Do the costs and benefits of fungal endophyte symbiosis vary with light availability? New Phytol. 188(3):824–834. doi:10.1111/j.1469-8137.2010.03428.x.

Deckmyn G, Laureysens I, Garcia J, Muys B, Ceulemans R. 2004. Poplar growth and yield in short rotation coppice: Model simulations using the process model SECRETS. Biomass and Bioenergy. 26(3):221–227. doi:10.1016/S0961-9534(03)00121-1.

Devireddy AR, Zandalinas SI, Gómez-Cadenas A, Blumwald E, Mittler R. 2018. Coordinating the overall stomatal response of plants: Rapid leaf-to-leaf communication during light stress. Sci Signal. 11(518). doi:10.1126/scisignal.aam9514.

Doty SL, Freeman JL, Cohu CM, Burken JG, Firrincieli A, Simon A, Khan Z, Isebrands JG, Lukas J, Blaylock MJ. 2017. Enhanced Degradation of TCE on a Superfund Site Using Endophyte- Assisted Poplar Tree Phytoremediation. doi:10.1021/acs.est.7b01504.

Doty SL, Oakley B, Xin G, Kang JW, Singleton G, Khan Z, Vajzovic A, Staley JT. 2009. Diazotrophic endophytes of native black cottonwood and willow. Symbiosis. 47(1):23–33. doi:10.1007/BF03179967.

Dunlap JM, Stettler RF. 2001. Variation in leaf epidermal and stomatal traits of Populus trichocarpa from two transects across the Washington Cascades. Can J Bot. 79(5):528–536. doi:10.1139/cjb-79-5-528.

Elmi AA, West CP. 1995. Endophyte infection effects on stomatal conductance, osmotic

adjustment and drought recovery of tall fescue. New Phytol. 131(1):61–67. doi:10.1111/j.1469-8137.1995.tb03055.x.

Fahlgren N, Ellsworth PZ, Cousins AB, Baxter I, Gehan MA, Feldman MJ. 2018. Components of Water Use Efficiency Have Unique Genetic Signatures in the Model C 4 Grass Setaria . Plant Physiol. 178(2):699–715. doi:10.1104/pp.18.00146.

Farquhar GD, Sharkey TD. 1982. Stomatal Conductance and Photosynthesis. Annu Rev Plant Physiol. 33(1):317–345. doi:10.1146/annurev.pp.33.060182.001533.

Feldman MJ, Paul RE, Banan D, Barrett JF, Sebastian J, Dinneny R, Yee M, Jiang H, Lipka AE, Brutnell TP, et al. 2017. Time dependent genetic analysis links field and controlled environment phenotypes in the model C 4 grass Setaria. PLoS Genet. 13(6):1–31.

Firrincieli A, Khorasani M, Frank AC, Doty SL. 2020. Influences of climate on phyllosphere endophytic bacterial communities of wild poplar. Front Plant Sci. 11(203):1–13. doi:10.3389/fpls.2020.00203.

Firrincieli A, Otillar R, Salamov A, Schmutz J, Khan Z, Redman RS, Fleck ND, Lindquist E, Grigoriev I V., Doty SL. 2015. Genome sequence of the plant growth promoting endophytic yeast Rhodotorula graminis WP1. Front Microbiol. 6(978):6–11. doi:10.3389/fmicb.2015.00978.

Flexas J, Bota J, Galmés J, Medrano H, Ribas-Carbó M. 2006. Keeping a positive carbon balance under adverse conditions: Responses of photosynthesis and respiration to water stress. Physiol Plant. 127(3):343–352. doi:10.1111/j.1399-3054.2006.00621.x.

Flexas J, Díaz-Espejo A, Conesa MA, Coopman RE, Douthe C, Gago J, Gallé A,

Galmés J, Medrano H, Ribas-Carbo M, et al. 2016. Mesophyll conductance to CO2 and Rubisco as targets for improving intrinsic water use efficiency in C3 plants. Plant Cell Environ. 39(5):965–982. doi:10.1111/pce.12622.

Garcia BJ, Labbé JL, Jones P, Abraham PE, Hodge I, Climer S, Jawdy S, Gunter L, Tuskan GA, Yang X, et al. 2018. Phytobiome and transcriptional adaptation of populus deltoides to acute progressive drought and cyclic drought. Phytobiomes J. 2(4):249–260. doi:10.1094/PBIOMES-04-18-0021-R.

Gornall JL, Guy RD. 2007. Geographic variation in ecophysiological traits of black cottonwood (Populus trichocarpa). Can J Bot. 85(12):1202–1213. doi:10.1139/B07-079.

Gottel NR, Castro HF, Kerley M, Yang Z, Pelletier DA, Podar M, Karpinets T, Uberbacher ED, Tuskan GA, Vilgalys R, et al. 2011. Distinct microbial communities within the endosphere and rhizosphere of Populus deltoides roots across contrasting soil types. Appl Environ Microbiol. 77(17):5934–5944. doi:10.1128/AEM.05255-11.

Heath KD, Podowski JC, Heniff S, Klinger CR, Burke P V., Weese DJ, Yang WH, Lau JA. 2020. Light availability and rhizobium variation interactively mediate the outcomes of legume–rhizobium symbiosis. Am J Bot. 107(2):229–238. doi:10.1002/ajb2.1435.

Henner DN, Hastings A, Pogson M, McNamara NP, Davies CA, Smith P. 2020. PopFor: A new model for estimating poplar yields. Biomass and Bioenergy. 134(February):105470. doi:10.1016/j.biombioe.2020.105470. https://doi.org/10.1016/j.biombioe.2020.105470.

Hoagland DR, Arnon DI. 1950. Circular 347. Univ Calif Agric Exp Stn.:1884–1949.

Holliday JA, Zhou L, Bawa R, Zhang M, Oubida RW. 2016. Evidence for extensive

parallelism but divergent genomic architecture of adaptation along altitudinal and latitudinal gradients in Populus trichocarpa. New Phytol. 209(3):1240–1251. doi:10.1111/nph.13643.

Huang YL, Zimmerman NB, Arnold AE. 2018. Observations on the early establishment of foliar endophytic fungi in leaf discs and living leaves of a model woody angiosperm, populus trichocarpa (Salicaceae). J Fungi. 4(2). doi:10.3390/jof4020058.

Kandel SL, Herschberger N, Kim SH, Doty SL. 2015. Diazotrophic endophytes of poplar and willow for growth promotion of rice plants in nitrogen-limited conditions. Crop Sci. 55(4):1765–1772. doi:10.2135/cropsci2014.08.0570.

Kandel SL, Joubert PM, Doty SL. 2017. Bacterial endophyte colonization and distribution within plants. Microorganisms. 5(4):9–11. doi:10.3390/microorganisms5040077.

Kang JW, Khan Z, Doty SL. 2012. Biodegradation of trichloroethylene by an endophyte of hybird poplar. Appl Environ Microbiol. 78(9):3504–3507. doi:10.1128/AEM.06852-11.

Karlova R, Boer D, Hayes S, Testerink C. 2021. Root plasticity under abiotic stress. Plant Physiol. 187(3):1057–1070. doi:10.1093/plphys/kiab392.

Kaschuk G, Kuyper TW, Leffelaar PA, Hungria M, Giller KE. 2009. Are the rates of photosynthesis stimulated by the carbon sink strength of rhizobial and arbuscular mycorrhizal symbioses? Soil Biol Biochem. 41(6):1233–1244. doi:10.1016/j.soilbio.2009.03.005. http://dx.doi.org/10.1016/j.soilbio.2009.03.005.

Khan Z, Guelich G, Phan H, Redman R, Doty S. 2012. Bacterial and yeast endophytes from poplar and willow promote growth in crop plants and grasses. ISRN Agron.

2012:1–11. doi:10.5402/2012/890280.

Khan Z, Kandel SL, Ramos DN, Ettl GJ, Kim SH, Doty SL. 2015. Increased biomass of nursery-grown douglas-fir seedlings upon inoculation with diazotrophic endophytic consortia. Forests. 6(10):3582–3593. doi:10.3390/f6103582.

Khan Z, Rho H, Firrincieli A, Hung SH, Luna V, Masciarelli O, Kim SH, Doty SL. 2016. Growth enhancement and drought tolerance of hybrid poplar upon inoculation with endophyte consortia. Curr Plant Biol. 6:38–47. doi:10.1016/j.cpb.2016.08.001. http://dx.doi.org/10.1016/j.cpb.2016.08.001.

Knoth JL, Kim SH, Ettl GJ, Doty SL. 2013. Effects of cross host species inoculation of nitrogen-fixing endophytes on growth and leaf physiology of maize. GCB Bioenergy. 5(4):408–418. doi:10.1111/gcbb.12006.

Knoth JL, Kim SH, Ettl GJ, Doty SL. 2014. Biological nitrogen fixation and biomass accumulation within poplar clones as a result of inoculations with diazotrophic endophyte consortia. New Phytol. 201(2):599–609. doi:10.1111/nph.12536.

Kumar V, Jain L, Jain SK, Chaturvedi S, Kaushal P. 2020. Bacterial endophytes of rice (Oryza sativa L.) and their potential for plant growth promotion and antagonistic acitivites. South African Journal of Botany. 134: 50-63. https://doi.org/10.1016/j.sajb.2020.02.017

Lawson T, Vialet-Chabrand S. 2019. Speedy stomata, photosynthesis and plant water use efficiency. New Phytol. 221(1):93–98. doi:10.1111/nph.15330.

Le J, Liu XG, Yang KZ, Chen XL, Zou JJ, Wang HZ, Wang M, Vanneste S, Morita M, Tasaka M, et al. 2014. Auxin transport and activity regulate stomatal patterning and

development. Nat Commun. 5:1–8. doi:10.1038/ncomms4090.

Leakey ADB, Ferguson JN, Pignon CP, Wu A, Jin Z, Hammer GL, Lobell DB. 2019. Water use efficiency as a constraint and target for improving the resilience and productivity of C3 and C4 crops. Annu Rev Plant Biol. 70:781–808. doi:10.1146/annurev-arplant-042817-040305.

van der Lelie D, Taghavi S, Monchy S, Schwender J, Miller L, Ferrieri R, Rogers A, Wu X, Zhu W, Weyens N, et al. 2009. Poplar and its bacterial endophytes: Coexistence and harmony. CRC Crit Rev Plant Sci. 28(5):346–358. doi:10.1080/07352680903241204.

Lima VF, Medeiros DB, Dos Anjos L, Cago J, Fernie AR, Daloso DM. 2018. Toward multifaceted roles of sucrose in the regulation of stomatal movement. Plant Signaling Behavior. 13(8). https://doi.org/10.1080/15592324.2018.1494468

Liu H, Carvalhais LC, Crawford M, Singh E, Dennis PG, Pieterse CMJ, Schenk PM. 2017. Inner plant values: Diversity, colonization and benefits from endophytic bacteria. Front Microbiol. 8(DEC):1–17. doi:10.3389/fmicb.2017.02552.

Liu Y, El-Kassaby YA. 2019. Phenotypic plasticity of natural Populus trichocarpa populations in response to temporally environmental change in a common garden. BMC Evol Biol. 19(1):1–15. doi:10.1186/s12862-019-1553-6.

Ma L, Rocha FI, Lee J, Choi J, Tejera M, Sooksa-Nguan T, Boersma N, VanLoocke A, Heaton E, Howe A. 2021. The impact of stand age and fertilization on the soil microbiome of miscanthus × giganteus. Phytobiomes J. 5(1):51–59. doi:10.1094/PBIOMES-01-20-0014-FI.

Matthews JSA, Vialet-Chabrand S, Lawson T. 2018. Acclimation to fluctuating light

impacts the rapidity of response and diurnal rhythm of stomatal conductance. Plant Physiol. 176(3):1939–1951. doi:10.1104/pp.17.01809.

Mattupalli C, Seethepalli A, York LM, Young CA. 2019. Digital imaging to evaluate root system architectural changes associated with soil biotic factors. Phytobiomes J. 3(2):102–111. doi:10.1094/PBIOMES-12-18-0062-R.

McAusland L, Vialet-Chabrand S, Davey P, Baker NR, Brendel O, Lawson T. 2016. Effects of kinetics of light-induced stomatal responses on photosynthesis and water-use efficiency. New Phytol. 211(4):1209–1220. doi:10.1111/nph.14000.

McKown AD, Guy RD. 2018. Hybrid vigour – Poplars play it cool. Tree Physiol. 38(6):785–788. doi:10.1093/treephys/tpy055.

Mckown AD, Guy RD, Klápště J, Geraldes A, Friedmann M, Cronk QCB, El-kassaby YA, Mansfield SD, Douglas CJ, Geraldes A, et al. 2014. Geographical and environmental gradients shape phenotypic trait variation and genetic structure in Populus trichocarpa. 201(4):1263–1276.

McKown AD, Klápště J, Guy RD, Corea ORA, Fritsche S, Ehlting J, El-Kassaby YA, Mansfield SD. 2019. A role for SPEECHLESS in the integration of leaf stomatal patterning with the growth vs disease trade-off in poplar. New Phytol. 223(4):1888–1903. doi:10.1111/nph.15911.

Mckown AD, Klápště J, Guy RD, Geraldes A, Porth I, Hannemann J, Friedmann M, Muchero W, Tuskan GA, Ehlting J, et al. 2014. Genome-wide association implicates numerous genes underlying ecological trait variation in natural populations of Populus trichocarpa. New Phytol. 203(2):535–553. doi:10.1111/nph.12815.

Medeiros DB, Souza LP, Antunes WC, Araujo WL, Daloso DM, Fernie AR. 2018. Sucrose breakdown within guard cells provides substrates for glycolysis and glutamine biosynthesis during the light-induced stomatal opening. Plant Journal. 94:583-594. 10.1111/tpj.13889

Morales Moreira ZP, Helgason BL, Germida JJ. 2021. Environment has a stronger effect than host plant genotype in shaping spring brassica napus seed microbiomes. Phytobiomes J. 5(2):220–230. doi:10.1094/PBIOMES-08-20-0059-R.

Morris CE. 2018. Phytobiomes contribute to climate processes that regulate temperature, wind, cloud cover, and precipitation. Phytobiomes J. 2(2):55–61. doi:10.1094/PBIOMES-12-17-0050-P.

Nogales A, Nobre T, Valadas V, Ragonezi C, Döring M, Polidoros A, Arnholdt-Schmitt B. 2016. Can functional hologenomics aid tackling current challenges in plant breeding? Brief Funct Genomics. 15(4):288–297. doi:10.1093/bfgp/elv030.

Pignon CP, Fernandes SB, Valluru R, Bandillo N, Lozano R, Buckler E, Gore MA, Long SP, Brown PJ, Leakey ADB. 2021. Phenotyping stomatal closure by thermal imaging for GWAS and TWAS of water use efficiency-related genes. Plant Physiol. 187(4):254–2562. doi:10.1093/plphys/kiab395.

Pignon CP, Leakey ADB, Long SP, Kromdijk J. 2021. Drivers of natural variation in water-use efficiency under fluctuating light are promising targets for improvement in sorghum. Front Plant Sci. 12:1–16. doi:10.3389/fpls.2021.627432.

Rho H, Doty SL, Kim SH. 2018. Estimating microbial respiratory CO2 from endophytic bacteria in rice. Plant Signal Behav. 13(8). doi:10.1080/15592324.2018.1500067.

Rho H, Doty SL, Kim SH. 2020. Endophytes alleviate the elevated CO2-dependent decrease in photosynthesis in rice, particularly under nitrogen limitation. J Exp Bot. 71(2):707–718. doi:10.1093/jxb/erz440.

Rho H, van Epps V, Wegley N, Doty SL, Kim SH. 2018. Salicaceae endophytes modulate stomatal behavior and increase water use efficiency in rice. Front Plant Sci. 9(188):1–15. doi:10.3389/fpls.2018.00188.

Rho H, Hsieh M, Kandel SL, Cantillo J, Doty SL, Kim SH. 2018. Do endophytes promote growth of host plants under stress? A meta-analysis on plant stress mitigation by endophytes. Microb Ecol. 75(2):407–418. doi:10.1007/s00248-017-1054-3.

Rogers A, McDonald K, Muehlbauer MF, Hoffman A, Koenig K, Newman L, Taghavi S, Van Der Lelie D. 2012. Inoculation of hybrid poplar with the endophytic bacterium Enterobacter sp. 638 increases biomass but does not impact leaf level physiology. GCB Bioenergy. 4(3):364–370. doi:10.1111/j.1757-1707.2011.01119.x.

Sanchez-Azofeifa A, Oki Y, Fernandes GW, Ball RA, Gamon J. 2012. Relationships between endophyte diversity and leaf optical properties. Trees - Struct Funct. 26(2):291–299. doi:10.1007/s00468-011-0591-5.

Sapp J. 2004. The dynamics of symbiosis: An historical overview. Can J Bot. 82(8):1046–1056. doi:10.1139/B04-055.

Sevanto S, Mcdowell NG, Dickman LT, Pangle R, Pockman WT. 2014. How do trees die? A test of the hydraulic failure and carbon starvation hypotheses. Plant, Cell Environ. 37(1):153–161. doi:10.1111/pce.12141.

Shakya M, Gottel N, Castro H, Yang ZK, Gunter L, Labbé J, Muchero W, Bonito G,

Vilgalys R, Tuskan G, et al. 2013. A multifactor analysis of fungal and bacterial community structure in the root microbiome of mature Populus deltoides trees. PLoS One. 8(10). doi:10.1371/journal.pone.0076382.

Sharkey TD, Raschke K. 1981. Separation and measurement of direct and indirect effects of light on stomata. Plant Physiol. 68(1):33–40. doi:10.1104/pp.68.1.33.

Soolanayakanahally RY, Guy RD, Silim SN, Drewes EC, Schroeder WR. 2009. Enhanced assimilation rate and water use efficiency with latitude through increased photosynthetic capacity and internal conductance in balsam poplar (Populus balsamifera L.). Plant, Cell Environ. 32(12):1821–1832. doi:10.1111/j.1365-3040.2009.02042.x.

Sparks JP, Black RA. 1999. Regulation of water loss in populations of Populus trichocarpa: The role of stomatal control in preventing xylem cavitation. Tree Physiol. 19(7):453–459. doi:10.1093/treephys/19.7.453.

Swarthout D, Harper E, Judd S, Gonthier D, Shyne R, Stowe T, Bultman T. 2009. Measures of leaf-level water-use efficiency in drought stressed endophyte infected and non-infected tall fescue grasses. Env and Exp Bot. 66: 88-93. doi:10.1016/j.envexbot.2008.12.002

Taghavi S, Garafola C, Monchy S, Newman L, Hoffman A, Weyens N, Barac T, Vangronsveld J, Van Der Lelie DD. 2009. Genome survey and characterization of endophytic bacteria exhibiting a beneficial effect on growth and development of poplar trees. Appl Environ Microbiol. 75(3):748–757. doi:10.1128/AEM.02239-08.

Talbott LD, Zeiger E. 1998. The role of sucrose in guard cell osmoregulation. J Exp Bot.

49:329-337.

Timm CM, Carter KR, Carrell AA, Jun S, Jawdy SS, Vélez JM, Gunter LE, Yang Z, Nookaew I, Engle NL, et al. 2018. Abiotic stresses shift belowground Populus associated bacteria toward a core stress microbiome. 3(1):1–17. doi:https://doi.org/10.1128/mSystems.00070-17.

Trivedi P, Leach JE, Tringe SG, Sa T, Singh BK. 2020. Plant–microbiome interactions: from community assembly to plant health. Nat Rev Microbiol. 18(11):607–621. doi:10.1038/s41579-020-0412-1. http://dx.doi.org/10.1038/s41579-020-0412-1.

Tuskan GA. 1998. Short-rotation woody crop supply systems in the United States: What do we know and what do we need to know? Biomass and Bioenergy. 14(4):307–315. doi:10.1016/S0961-9534(97)10065-4.

Underwood W, Melotto M, He SY. 2007. Role of plant stomata in bacterial invasion. Cell Microbiol. 9(7):1621–1629. doi:10.1111/j.1462-5822.2007.00938.x.

Varga T, Hixson KK, Ahkami AH, Sher AW, Barnes ME, Chu RK, Battu AK, Nicora CD, Winkler TE, Reno LR, et al. 2020. Endophyte-promoted phosphorus solubilization in Populus. Front Plant Sci. 11(567918). doi:10.3389/fpls.2020.567918.

Wagner MR, Lundberg DS, Del Rio TG, Tringe SG, Dangl JL, Mitchell-Olds T. 2016. Host genotype and age shape the leaf and root microbiomes of a wild perennial plant. Nat Commun. 7. doi:10.1038/ncomms12151.

Wang D, Le Bauer D, Dietze M. 2013. Predicting yields of short-rotation hybrid poplar (Populus spp.) for the United States through model-data synthesis. Ecol Appl. 23(4):944–958. doi:10.1890/12-0854.1.

Weyens N, van der Lelie D, Taghavi S, Newman L, Vangronsveld J. 2009. Exploiting plant-microbe partnerships to improve biomass production and remediation. Trends Biotechnol. 27(10):591–598. doi:10.1016/j.tibtech.2009.07.006.

Wickham H (2016). *ggplot2: Elegant Graphics for Data Analysis*. Springer-Verlag New York. ISBN 978-3-319-24277-4, https://ggplot2.tidyverse.org.

Whitham TG, Young WP, Martinsen GD, Gehring CA, Schweitzer JA, Shuster SM, Wimp GM, Fischer DG, Bailey JK, Lindroth RL, et al. 2003. Community and ecosystem genetics: A consequence of the extended phenotype. Ecology. 84(3):559–573. doi:10.1890/0012-9658(2003)084[0559:CAEGAC]2.0.CO;2.

Weisberg FJ. 2019. An R companion to applied regression, Third edition. Sage, Thousand Oaks. https://socialsciences.mcmaster.ca/jfox/Books/Companion/.

Wipf HML, Bùi TN, Coleman-Derr D. 2021. Distinguishing between the impacts of heat and drought stress on the root microbiome of sorghum bicolor. Phytobiomes J. 5(2):166–176. doi:10.1094/PBIOMES-07-20-0052-R.

Xin G, Glawe D, Doty SL. 2009. Characterization of three endophytic , indole-3-acetic acid- producing yeasts occurring in Populus trees. Mycol Res. 113(9):973–980. doi:10.1016/j.mycres.2009.06.001.

Xin G, Zhang G, Kang JW, Staley JT, Doty SL. 2009. A diazotrophic , indole-3-acetic acid-producing endophyte from wild cottonwood. Biol Fertil Soils. 45:669–674. doi:10.1007/s00374-009-0377-8.

Zhang M, Suren H, Holliday JA, Gaut B. 2019. Phenotypic and genomic local adaptation across latitude and altitude in Populus trichocarpa. Genome Biol Evol. 11(8):2256–

2272. doi:10.1093/gbe/evz151.

TABLES

Table 1: Summary of endophytes used in consortium.

Strain	Species (original isolation source)	Characteristics
WP5 [a, b]	*Rahnella aceris* (wild poplar, *P. trichocarpa*)	N-fixation, P-solubilization, trehalose production, PQQ antioxidant production
WW5 [b]	*Sphingobium sp.* (wild willow, *Salix sitchensis*)	High performer in agricultural field trials
WP1 [c, d]	*Rhodotorula graminis* (wild poplar, *P. trichocarpa*)	IAA production, root induction, trehalose production, butane-2,3-diol production
WPB [e]	*Burkholderia vietnamiensis* (wild poplar, *P. trichocarpa*)	N-fixation, ACC deaminase, trehalose production
PDN3 [f, g]	*Enterobacter asburiae* (hybrid poplar, *P. deltoides* x *P. nigra* OP-367)	IAA production, butane-2,3-diol production, high performance in TCE phytoremediation

References:

[a] (Varga et al. 2020); [b] (Doty et al. 2009); [c] (Xin, Glawe, et al. 2009); [d] (Firrincieli et al. 2015); [e] (Xin, Zhang, et al. 2009); [f] (Kang et al. 2012); [g] (Doty et al. 2017)

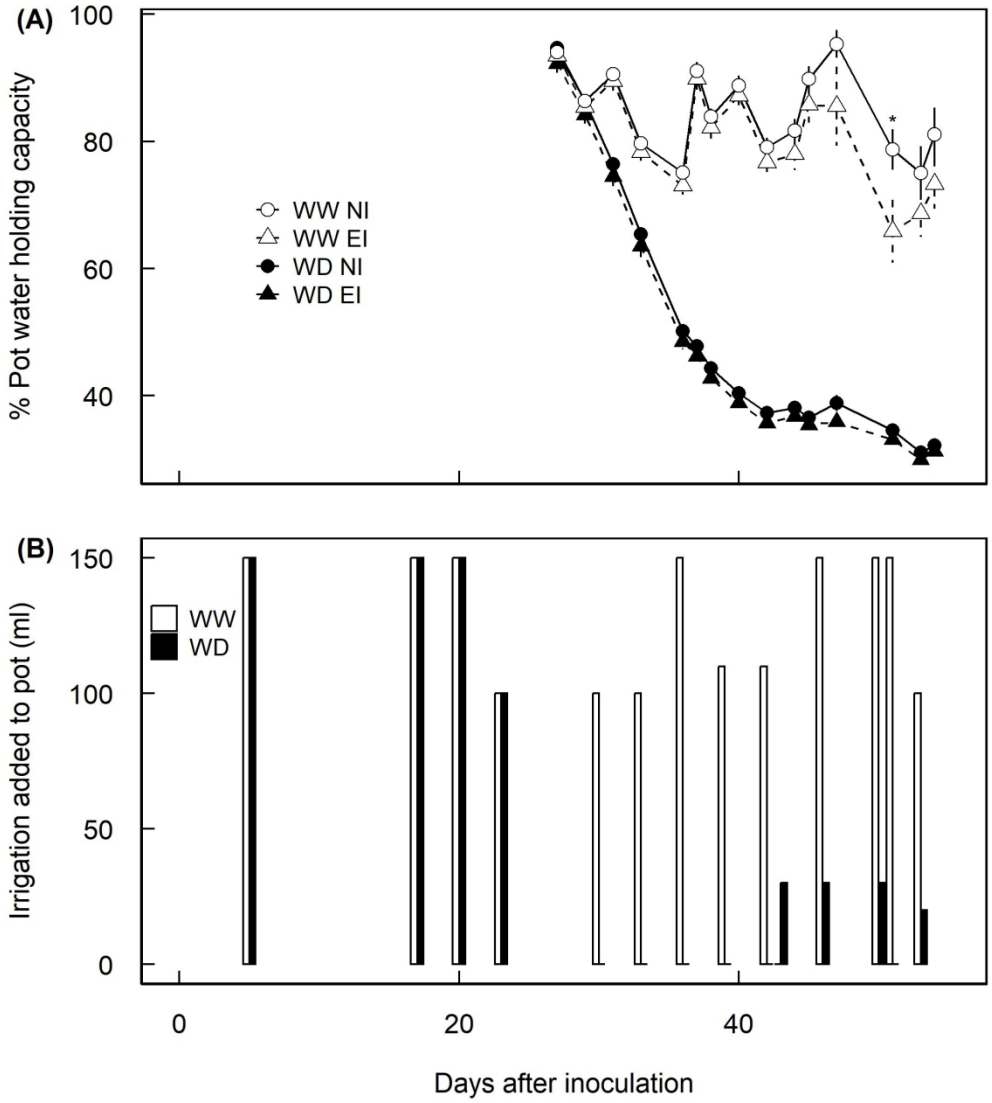

Figure 1: Well-watered and water-deficit treatment progression expressed as a percentage of pot water holding capacity (A). The amount of irrigation applied as water or nutrient solution applied to well-watered pots (open bars) and water-deficit pots (filled bars) (B). In (A), points represent treatment means and vertical bars represent their standard error at each timepoint. Stars (*) indicate significant NI versus EI treatment differences (Welch's two-sample t-test, p-value < 0.05) within an abiotic condition at a given timepoint. Abbreviations: WW NI, well-watered non-inoculated; WW EI, well-watered endophyte-inoculated; WD NI, water-deficit non-inoculated; WD EI, water-deficit endophyte-inoculated.

179x199mm (300 x 300 DPI)

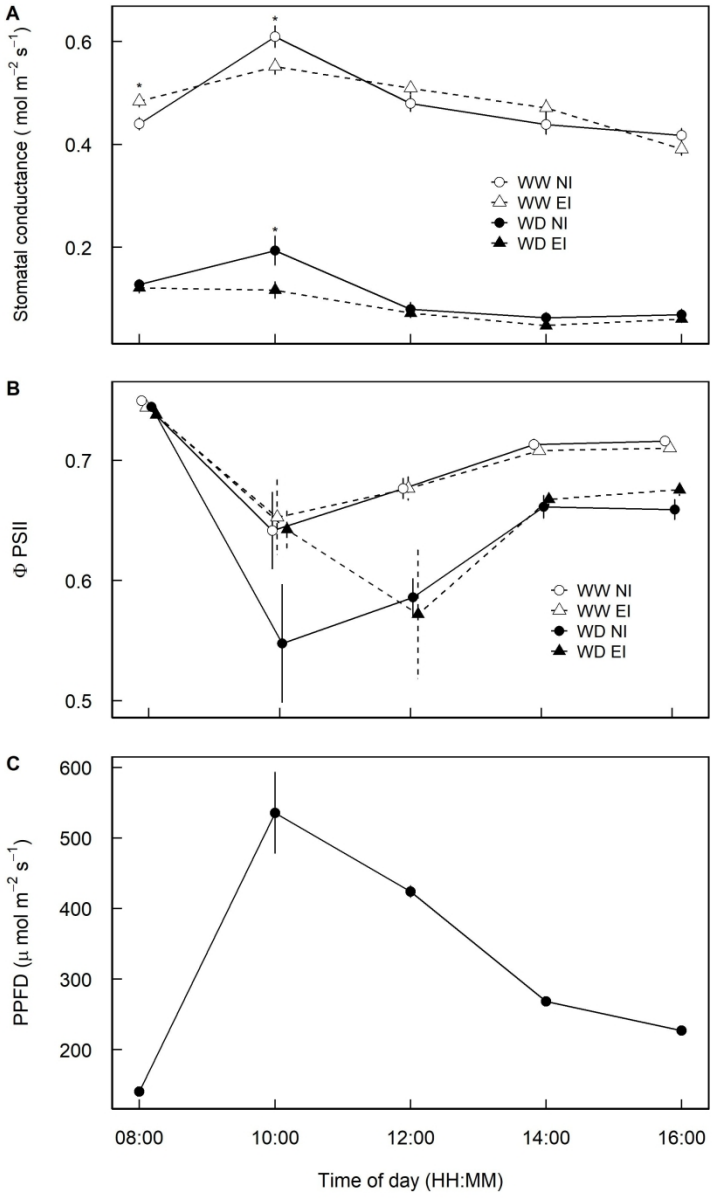

Figure 2: Diurnal course of stomatal conductance (A), ΦPSII (B), and photosynthetically active photon flux density (PPFD, C). Stars (*) indicate significant NI versus EI treatment differences (Welch's two sample t-test, p-value < 0.05) within an abiotic condition at a given timepoint. In (A) and (B), points represent treatment means and vertical bars present their standard error. In (B), points are offset above each timepoint to improve visibility between treatments. In (C), points and vertical bars represent the mean and standard error, respectively, of all observations. Abbreviations: WW NI, well-watered non-inoculated; WW EI, well-watered endophyte-inoculated; WD NI, water-deficit non-inoculated; WD EI, water-deficit endophyte-inoculated.

179x299mm (300 x 300 DPI)

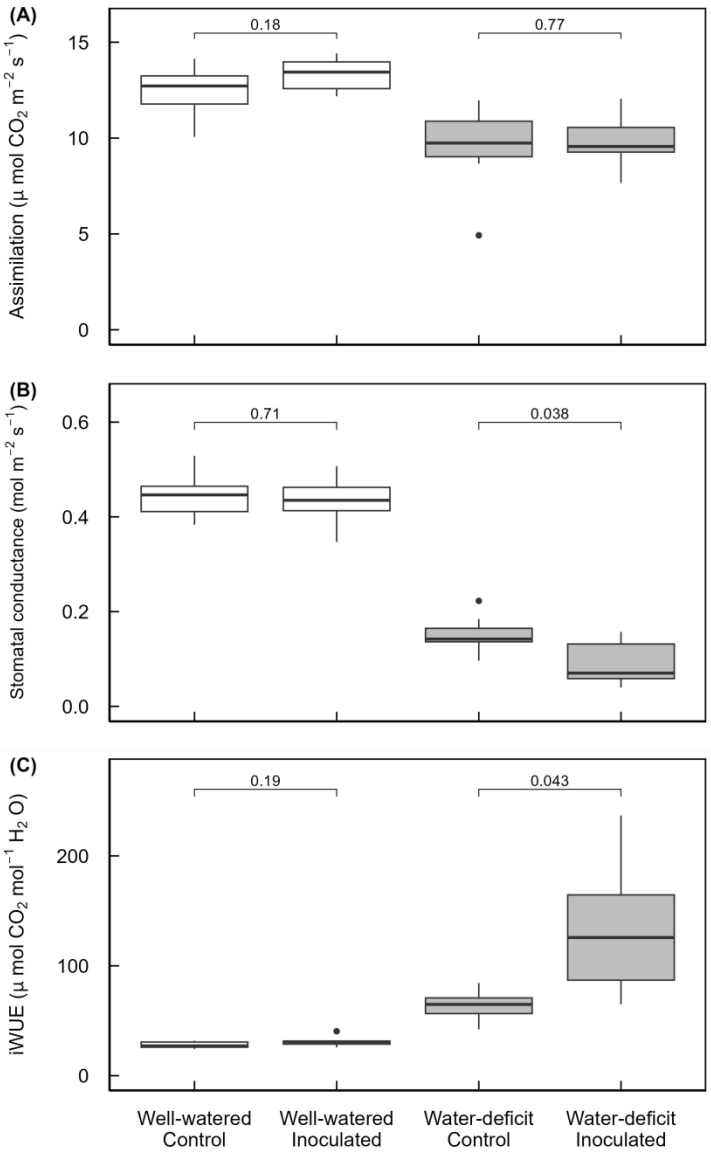

Figure 3: Net assimilation rate (A), stomatal conductance (B), and intrinsic water use efficiency (iWUE, C) measured at 10:30 54 days after inoculation. In each panel, the left two boxplots (open) represent well-watered plants and the right two boxplots (filled) represent water-deficit plants. Within each well-watered and water-deficit pair, non-inoculated plants are on the left and inoculated plants are on the right. The horizontal bars above each well-watered and water-deficit pair indicate the p-value from a Welch's two-sample t-test between non-inoculated and inoculated treatments.

179x299mm (300 x 300 DPI)

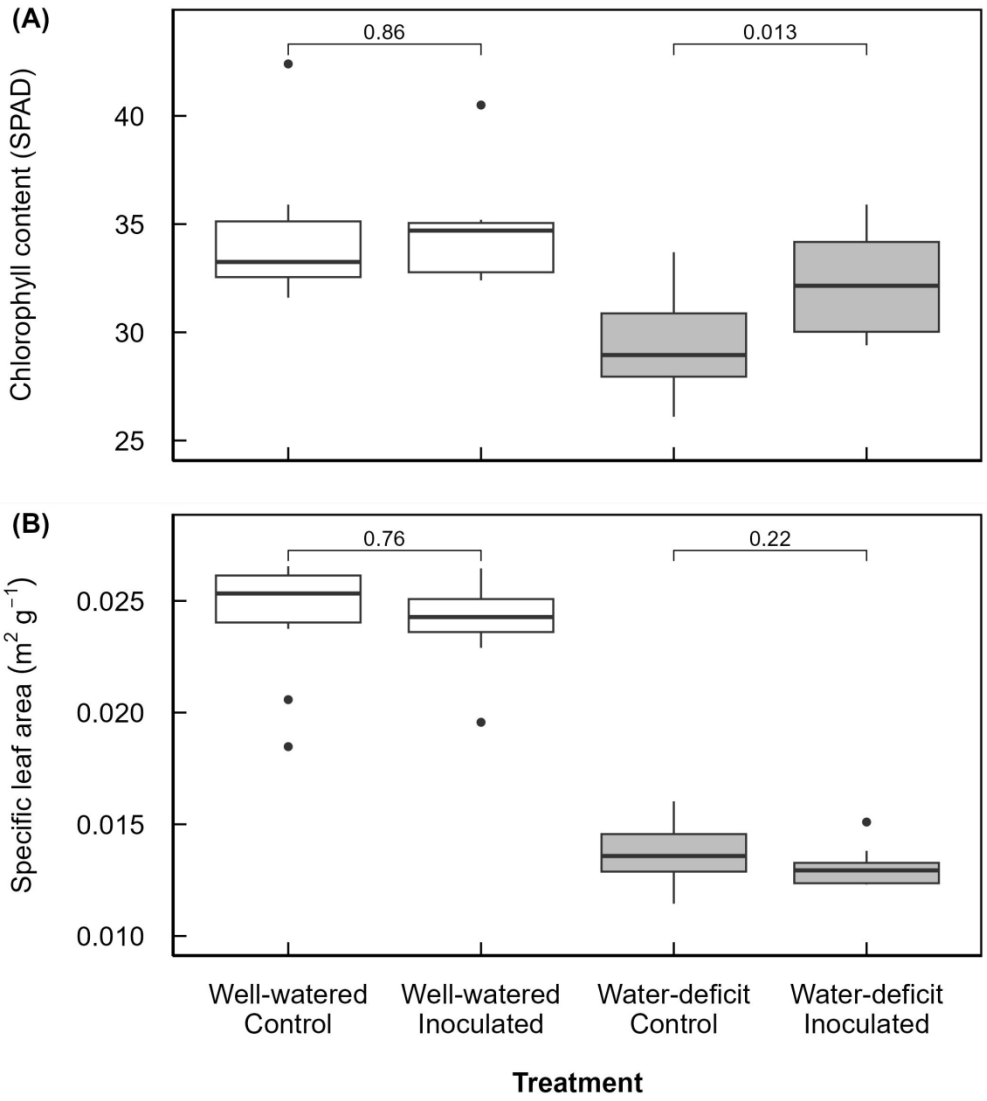

Figure 4: Leaf chlorophyll content (A) and specific leaf area (B). In each panel, the left two boxplots (open) represent well-watered plants and the right two boxplots (filled) represent water-deficit plants. Within each well-watered and water-deficit pair, non-inoculated plants are on the left and inoculated plants are on the right. The horizontal bars above each well-watered and water-deficit pair indicate the p-value from a Welch's two-sample t-test between non-inoculated and inoculated treatments.

179x199mm (300 x 300 DPI)

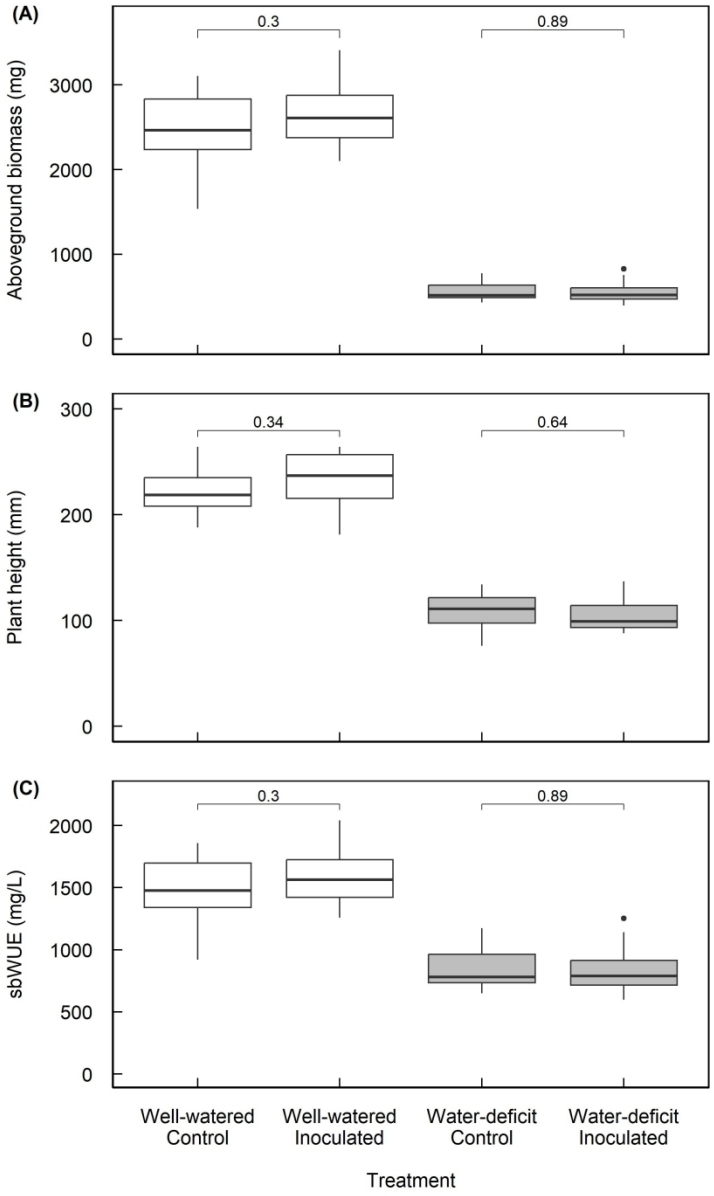

Figure 5: Aboveground biomass (A), plant height (B), and shoot biomass water use efficiency (sbWUE, C). In each panel, the left two boxplots (open) represent well-watered plants and the right two boxplots (filled) represent water-deficit plants. Within each well-watered and water-deficit pair, non-inoculated plants are on the left and inoculated plants are on the right. The horizontal bars above each well-watered and water-deficit pair indicate the p-value from a Welch's two-sample t-test between non-inoculated and inoculated plants.

179x299mm (300 x 300 DPI)

Supplemental Table 1. Mean values of diurnal stomatal conductance (g_{sw}, mol m^{-2} s^{-1}) measurements, ANOVA model outputs, and two-sample Welch's t-test results. Bolded and italicized text highlights p-values <0.05; italicized text highlights p-values < 0.1.

		Parameter				
	Treatment	gsw 08:00	gsw 10:00	gsw 12:00	gsw 14:00	gsw 16:00
Mean value:	WW NI	0.4402605	0.6095356	0.4795263	0.4388809	0.4176574
	WW EI	0.4844155	0.5516446	0.5094648	0.4713549	0.3913324
	WD NI	0.1277926	0.1938634	0.0797912	0.0631823	0.068931
	WD EI	0.1213462	0.116884	0.0721945	0.0477375	0.0605926
Two-way ANOVA:	Inoc (df 1)	*3.482 (0.073)*	***9.681 (0.004)***	0.887 (0.355)	0.494 (0.488)	2.380 (0.135)
F-value (p-value)	Water (df 1)	***1132.25 (< 2e-16)***	***384.92 (< 2.2e-16)***	***1245.05 (<2e-16)***	***1087.48 (< 2e-16)***	***914.43 (<2e-16)***
	Block (df 9)	1.457 (0.214)	0.735 (0.674)	1.608 (0.163)	*1.972 (0.084)*	0.850 (0.579)
	Interaction (df 1)	***6.293 (0.018)***	0.194 (0.663)	2.504 (0.125)	*3.908 (0.058)*	0.641 (0.430)
	Residuals (df 27)					
	Multiple R2	0.977	0.937	0.9791	0.9762	0.9716
Welch's t-test:	WW NI vs WW EI					
	t-statistic	2.7131	-2.2062	1.4984	1.327	-1.4505
	DF, adjusted	17.953	16.476	16.946	17.284	17.978
	p-value	***0.0147***	***0.04188***	0.1524	0.2018	0.1641
	WD NI vs WD EI					
	t-statistic	-0.47142	-2.358	-0.48137	-1.3477	-0.66651
	DF, adjusted	17.706	14.34	15.998	14.422	14.762
	p-value	0.6431	***0.033***	0.6368	0.1986	0.5154

Supplemental Table 2. Mean values of diurnal *ΦPSII* measurements, ANOVA model outputs, and two-sample Welch's t-test results. Bolded and italicized text highlights p-values <0.05; italicized text highlights p-values < 0.1.

		Parameter				
	Treatment	*ΦPSII* 8:00	*ΦPSII* 10:00	*ΦPSII* 12:00	*ΦPSII* 14:00	*ΦPSII* 16:00
Mean value:	WW NI	0.7496391	0.6415433	0.6765244	0.7131062	0.7160461
	WW EI	0.7441904	0.6526292	0.6765039	0.7080789	0.710136
	WD NI	0.7445046	0.5476703	0.5859933	0.6613151	0.6590065
	WD EI	0.737931	0.6424419	0.5718893	0.667471	0.6756339
Two-way ANOVA:	Inoc (df 1)	3.5221 (0.0714)	2.8901 (0.1006)	0.0601 (0.8082)	0.0087 (0.9263)	0.7898 (0.382)
F-value (p-value)	Water (df 1)	*3.1606 (0.0867)*	2.7928 (0.1062)	***11.46 (0.0021)***	***58.44 (3.187e-08)***	***57.62 (3.638e-08)***
	Block (df 9)	1.2184 (0.3247)	1.8253 (0.1094)	0.9756 (0.4812)	1.3956 (0.2388)	0.7462 (0.6644)
	Interaction (df 1)	0.0372 (0.8485)	1.8062 (0.1901)	0.0597 (0.8088)	0.8562 (0.3630)	*3.4928 (0.0725)*
	Residuals (df 27)					
	Multiple r2	0.1272	0.234	0.1766	0.6056	0.5922
Welch's t-test:	WW NI vs WW EI					
	t-statistic	-1.0722	0.24779	0.0015625	-0.83418	-1.0128
	DF, adjusted	17.689	17.977	17.719	17.69	17.988
	p-value	0.2981	0.8071	0.9988	0.4153	0.4153
	WD NI vs WD EI					
	t-statistic	-1.5637	1.8322	-0.25219	0.55238	1.6452
	DF, adjusted	16.658	10.765	10.565	14.788	15.018
	p-value	0.1367	*0.0947*	0.8057	0.8057	0.5889

Supplemental Table 3. Mean values of CO_2 assimilation rate (A_n, μmol m^{-2} s^{-1}), stomatal conductance (g_{sw}, mol m^{-2} s^{-1}), and intrinsic water use efficiency (*iWUE*, μmol mol^{-1}) measured on 10:00 54 DAI, ANOVA model outputs, and two-sample Welch's t-test results. Bolded and italicized text highlights p-values <0.05; italicized text highlights p-values < 0.1.

		Parameter		
	Treatment	A_n	g_{sw}	*iWUE*
Mean value:	WW NI	12.422488	0.44435679	28.08434
	WW EI	13.30642	0.43425013	31.05351
	WD NI	9.493875	0.15189654	63.7142
	WD EI	9.816574	0.09064756	134.11795
Two-way ANOVA:	Inoc (df 1)	1.7904 (0.1985)	1.8005 (0.1973)	***7.6734 (0.01310)***
F-value (p-value)	Water (df 1)	***33.61 (2.143e-05)***	***358.07 (7.381e-13)***	***33.08 (2.347e-05)***
	Block (df 6)	1.9427 (0.1316)	1.9491 (0.1305)	1.0803 (0.4124)
	Interaction (df 1)	0.2426 (0.6286)	1.6285 (0.2191)	***7.8959 (0.01205)***
	Residuals (df 17)			
	Multiple R2	0.7356	0.9334	0.6395781
Welch's t-test:	WW NI vs WW EI			
	t-statistic	1.4454	-0.37473	1.4203
	DF, adjusted	10.12	11.992	10.156
	p-value	0.1786	0.7144	0.1855
	WD NI vs WD EI			
	t-statistic	0.30369	-2.4001	2.6389
	DF, adjusted	10.354	9.6355	5.4113
	p-value	0.7674	***0.0381***	***0.0426***

Supplemental Table 4. Mean values of SPAD, specific leaf area (*SLA*, $mm^2\ mg^{-1}$), aboveground productivity (g), height (mm), and shoot biomass water use efficiency (WUE_{sb}, $mg\ L^{-1}$), ANOVA model outputs, and two-sample Welch's t-test results. Bolded and italicized text highlights p-values <0.05; italicized text highlights p-values < 0.1.

		Parameter				
	Treatment	SPAD	SLA	Aboveground productivity	Height	WUE_{sb}
Mean value:	WW NI	34.36	24.34427	2.448	222.6	1465.868
	WW EI	34.58	24.01836	2.67679	233.9	1602.868
	WD NI	29.37	13.72873	0.56428	108.4	854.9697
	WD EI	32.22	13.06517	0.55623	104.8	842.7727
Two-way ANOVA:	Inoc (df 1)	*3.614 (0.068)*	0.6934 (0.4123)	1.5198 (0.2282)	0.5212 (0.4765)	1.2927 (0.2655)
F-value (p-value)	Water (df 1)	***20.71 (0.0001)***	***329.48 (<2e-16)***	***500.12 (< 2.2e-16)***	***520.31 (< 2.2e-16)***	***155.99 (9.878e-13)***
	Block (df 9)	1.041 (0.4345)	0.8492 (0.5793)	***3.2128 (0.0089)***	***3.7074 (0.0038)***	***5.1138 (0.0004)***
	Interaction (df1)	2.653 (0.1149)	0.0807 (0.7785)	1.7496 (0.1970)	1.9514 (0.1738)	1.8474 (0.1853)
	Residuals (df 27)					
	Multiple R2	0.3844	0.8931	0.9303	0.9331	0.832
Welch's t-test:	WW NI vs WW EI					
	t-statistic	0.17638	-0.31223	1.0622	0.98134	1.0622
	DF, adjusted	16.707	15.944	17.765	17.608	17.765
	p-value	0.8621	0.7589	0.30204	0.3397	0.30204
	WD NI vs WD EI					
	t-statistic	2.7442	-1.2792	-0.13807	-0.47198	-0.13807
	DF, adjusted	17.984	15.25	17.357	19.669	17.357
	p-value	***0.0133***	0.22	0.8918	0.6427	0.8918